MALAYSIAN JOURNAL OF MICROSCOPY

Journal homepage: https://malaysianjournalofmicroscopy.org

RESEARCH ARTICLE

EFFECT OF FERRIHYDRITE-CHITOSAN NANOCOMPOSITES PRECURSOR RATIO ON PALM OIL MILL EFFLUENT PRE-TREATMENT

Juliana Jumadi[1], Azlan Kamari[1,*], Wan Haslinda Wan Ahmad[1], Norlaili Abu Bakar[1], Budi Hastuti[2], Is Fatimah[3], Eli Rohaeti[4]

[1]Department of Chemistry, Faculty of Science and Mathematics, Universiti Pendidikan Sultan Idris, 35900, Tanjong Malim, Perak, Malaysia.
[2]Department of Chemistry Education, Faculty of Teacher Training and Education, Universitas Sebelas Maret, Jl. Ir. Sutami 36A, Kentingan Surakarta 57126, Indonesia.
[3]Nanomaterials and Sustainable Chemistry Research Centre, Universitas Islam Indonesia, Chemistry Research Building, Kampus Terpadu UII, Jl. Kaliurang Km 14, Sleman, Yogyakarta 55584, Indonesia.
[4]Department of Chemistry Education, Faculty of Mathematics and Natural Sciences, Universitas Negeri Yogyakarta, Yogyakarta 55281, Indonesia.

Abstract. Statistically, it has been estimated that more than 0.50 tonnes of palm oil mill effluent (POME) will be generated for each tonne of fresh fruit bunches (FFBs) production. Fresh POME normally possesses a high amount of total solid, biochemical oxygen demand (BOD), chemical oxygen demand (COD), oil and grease (O&G). Therefore, POME treatment has received great attention from environmental scientists. In this study, ferrihydrite-chitosan (FC) nanocomposites were prepared using a simple co-precipitation method by varying the ratio of ferrihydrite and chitosan. The influence of precursor ratios (1:1, 2:1 and 1:2 w/w) of FC nanocomposites on palm oil mill effluent pre-treatment was investigated in flocculation studies at optimum experimental conditions. The characteristics of FC nanocomposites, before and after POME treatment were studied using Fourier transform infrared (FTIR) spectrometer, energy dispersive X-ray (EDX) spectrometer and optical polarising microscope (OPM) analyses. The results indicate that the 1:1 w/w FC nanocomposite exhibited the highest percentage of contaminant reduction at 82.63 %, 75.70 %, 74.07 % and 49.08 % for total suspended solids (TSS), turbidity, COD, and O&G removal, respectively. The synergistic effects between ferrihydrite and chitosan precursors highlight the potential of the FC nanocomposites as promising flocculants for POME. Overall, this research is relevant to POME management and treatment, particularly in Indonesia and Malaysia the two major palm oil producers in the world. Moreover, research findings support the sixth Sustainable Development Goal of the United Nations, namely Clean Water and Sanitation.

Keywords: Chitosan, ferrihydrite, ferrihydrite-chitosan nanocomposites, flocculant, palm oil mill effluent treatment.

Article Info

Received 7 December 2025
Accepted 23 April 2026
Published 8 June 2026

***Corresponding author: azlan.kamari@fsmt.upsi.edu.my**
Copyright Malaysian Journal of Microscopy (2026). All rights reserved.
ISSN: 1823-7010, eISSN: 2600-7444

1. INTRODUCTION

The discharge of palm oil mill effluent (POME) into water bodies without proper treatment is of great concern mainly because it contributes to eutrophication, which results in the overgrowth of algae and aquatic plants, leading to a depletion of oxygen and endangering aquatic life [1]. The uncontrolled release of POME on land can also result in soil contamination, adversely affecting soil structure and nutrient balance [2]. As a matter of fact, the presence of organic matter and potentially toxic compounds in POME poses a threat to aquatic ecosystems, causing harm to fish and other aquatic organisms and contributing to biodiversity loss. Moreover, methane emissions from untreated POME, a potent greenhouse gas, further exacerbate environmental concerns [3].

To mitigate the environmental impact of POME, it is crucial to implement effective wastewater treatment strategies that minimise these adverse effects and promote sustainability in the palm oil industry. Conventional treatment approaches, including anaerobic digestion and ponding systems have shown limitations in addressing the complex composition of POME [4]. Anaerobic digestion struggles with incomplete pollutant removal, long retention time, process instability, sludge accumulation and methane emission. Meanwhile, extensive land area requirement, prolonged treatment period, odour problem, poor process control, groundwater contamination and low treatment efficiency for emerging pollutants are normally associated with ponding system [4,5]. POME normally possesses high organic content, suspended solids and nutrient levels [5]. Recent research studies have shifted focus towards innovative technologies, with nanocomposites have been regarded as promising effective clean-up materials for POME treatment. Iron oxide and chitosan, possess unique attributes and have emerged as promising candidates for environmental remediation. Iron oxide, like ferrihydrite renowned for its magnetic properties and high surface reactivity that exhibits remarkable ability to capture contaminants and organic pollutants from water sources [6]. On the other hand, chitosan derived from crustacean shells, stands out as a biodegradable and renewable biopolymer with distinctive qualities, including antimicrobial properties and a notable affinity for metal ions [7].

The synergy and application of outstanding precursors in composite materials presents a promising strategy to enhance effluent treatment. Several studies have delved into the effects of precursor ratio on the performance of nanocomposites, emphasising the need for precision in composition for optimal functionality. A number of research works suggest that variations in precursor ratio significantly impact the structural and chemical properties of nanocomposites, influencing their affinity for specific contaminants [8]. However, information on the effect of ferrihydrite and chitosan precursors ratio on water treatment is still scarce. Most of previous research works, mainly focused on potential of ferrihydrite-chitosan composite as an adsorbent for metal ions and dyes. In fact, the feasibility of ferrihydrite-chitosan nanocomposite to treat POME has never been reported in the literature. The first attempt to evaluate the applicability of ferrihydrite-chitosan nanocomposite as a flocculant for POME treatment was reported in our previous study [9].

Therefore, the ultimate aim of this study was to unlock the full potential of ferrihydrite-chitosan (FC) nanocomposites and tailor their composition for the specific challenges presented by POME. The complex interrelationship between the precursor ratio of ferrihydrite and chitosan (1:1, 2:1 and 1:2 w/w) in the preparation of FC nanocomposites and their feasibility as flocculants to reduce turbidity, TSS, COD and O&G of POME were investigated. To accomplish this, experiments were carried out to determine the optimal flocculation conditions. This investigation is imperative in order to optimise the adsorption capacity and overall effectiveness of the nanocomposites in the remediation of POME. Our study not only aim to unveil the potential of FC nanocomposites, but also to emphasise the critical role that precursor ratio plays in unlocking their full potential. By examining the physicochemical properties of the nanocomposites, comprehensive insights that contribute to understanding of FC nanocomposites will be provided.

2. MATERIALS AND METHODS

2.1 Materials

Analytical grade chemicals were used in this study. Chitosan powder with 99 % degree of deacetylation was purchased from Acros Organic, United States of America. Iron(III) chloride hexahydrate was obtained from Bendosen Laboratory Chemicals, Malaysia. Ferrihydrite powder was supplied by Nanochemazone, Malaysia. Aluminium Sulfate (Alum) and Sodium Dodecyl Sulfate (SDS) surfactant were purchased from Fisher Scientific, United States of America. Fresh raw POME samples were collected at a palm oil processing plant situated in Trolak, Perak, Malaysia (3°56'20.99"N, 101°21'06.92"E). Polyethylene bottles containing POME samples were kept at 4 °C. This precautionary measure is imperative particularly to avoid biodegradation of POME caused by microorganisms and to assist in maintaining the integrity of the POME sample for subsequent analyses.

2.2 Preparation of FC Nanocomposites

The FC nanocomposites with the size of 10 to 20 nm were synthesised at three weight ratios, namely 1:1, 2:1 and 1:2 as described in our previous study [9]. Briefly, a mixture solution containing SDS (2.0 g) and ferrihydrite powder (0.25 g) was prepared in 400 mL of deionised water. Chitosan solution, prepared with 0.25 g of chitosan powder in 100 mL of acetic acid (1 % w/v), was then dropped slowly into SDS and ferrihydrite mixture solution. The mixture was stirred (200 rpm) at room temperature (26 ± 1 °C) for 1 h. This reaction produced precipitates. The precipitates were then separated, carefully washed with deionised water and ethanol, and dried in an oven set at 55 °C. For 2:1 and 1:2 w/w FC nanocomposites, the preparation steps were similar to that of 1:1 w/w FC nanocomposites using appropriate amount of ferrihydrite and chitosan precursors.

2.3 Characterisation of FC Nanocomposites

In the investigation of the properties of nanocomposites, the presence of functional groups and potential reactive sites was examined using a Thermo Nicolet 6700 FTIR Spectrometer coupled with a Platinum Diamond Attenuated Total Reflectance (ATR) disc. The FTIR spectra were obtained at wavenumber range of 4000 to 400 cm^{-1} with 3 cm^{-1} resolution and 35 cumulative scans. A Hitachi SU 8020 UHR Field Emission Scanning Electron Microscope equipped with an EDX spectrometer was used to determine the elemental composition of the nanocomposites. The surface of each sample was coated with a thin layer of platinum using a Horiba vacuum electric sputter to avoid complication due to charging. A tungsten filament was set at 20.0 kV for EDX analysis. To visualise the surface property of POME sample, OPM analysis was performed before and after treatment with FC nanocomposites. A small amount of POME was placed on a microscope slide and the images were observed using a Nikon LV100 OPM with an attached digital video Olympus camera for real-time visualisation.

2.4 Flocculation Studies

Generally, the flocculant was added to POME sample in 500 mL Erlenmeyer flask. The mixture was then stirred at 250 rpm for 3 min to ensure uniform distribution. The stirring speed was subsequently reduced to 50 rpm for an additional 30 min, aimed at fostering increased floc production through enhanced particle collision. Over the next 75 min, the system settled under the influence of an external magnetic field. The measurements of turbidity, TSS, COD and O&G were determined to ascertain final concentrations. The experiments were performed in triplicates at room temperature ranged from 25 to 28 °C. The samples underwent separation to filter FC nanocomposites settled at 2 cm under water surface following flocculation treatment.

2.5 Methods for POME Analysis

The physicochemical parameters of the POME utilised in the flocculation treatment experiments were analysed using analytical methods recommended by the APHA Standard Methods

for the Examination of Water and Wastewater. The initial characteristics of the POME were determined as: pH (4.67 ± 0.05) measured using a Thermo Scientific Orion 2-star pH meter, turbidity (37,450 ± 1,040 NTU) measured using a Hach 2100P turbidimeter, TSS (19,694 ± 714 mg L^{-1}) determined through 2540D drying at 103-105 °C method, O&G (6,166 ± 261 mg L^{-1}) analysed using a hexane extractable gravimetric method and COD (60,100 ± 3,460 mg L^{-1}) measured using 5220 COD method. These analytical techniques provide a comprehensive understanding of the initial composition of the POME, essential for evaluating the effectiveness of the subsequent treatment processes.

3. RESULTS AND DISCUSSION

3.1 Flocculation Studies

Determining the optimal dosage is a critical factor in establishing the most effective conditions for application of iron oxide-chitosan nanocomposites in the flocculation process. As highlighted by Saritha et al. [10], improper dosing either insufficient or excessive, can lead to suboptimal performance in the treatment procedure. The main objective was to identify the dosage that minimises costs while maximising treatment efficiency. In this study, the influence of flocculant dosage on removal percentage was assessed in the range between 0.50 and 2.5 g L^{-1}. The flocculation system was carried out for 75 min with original POME pH value. Figure 1 illustrates the dosage-dependent variations in treatment outcomes.

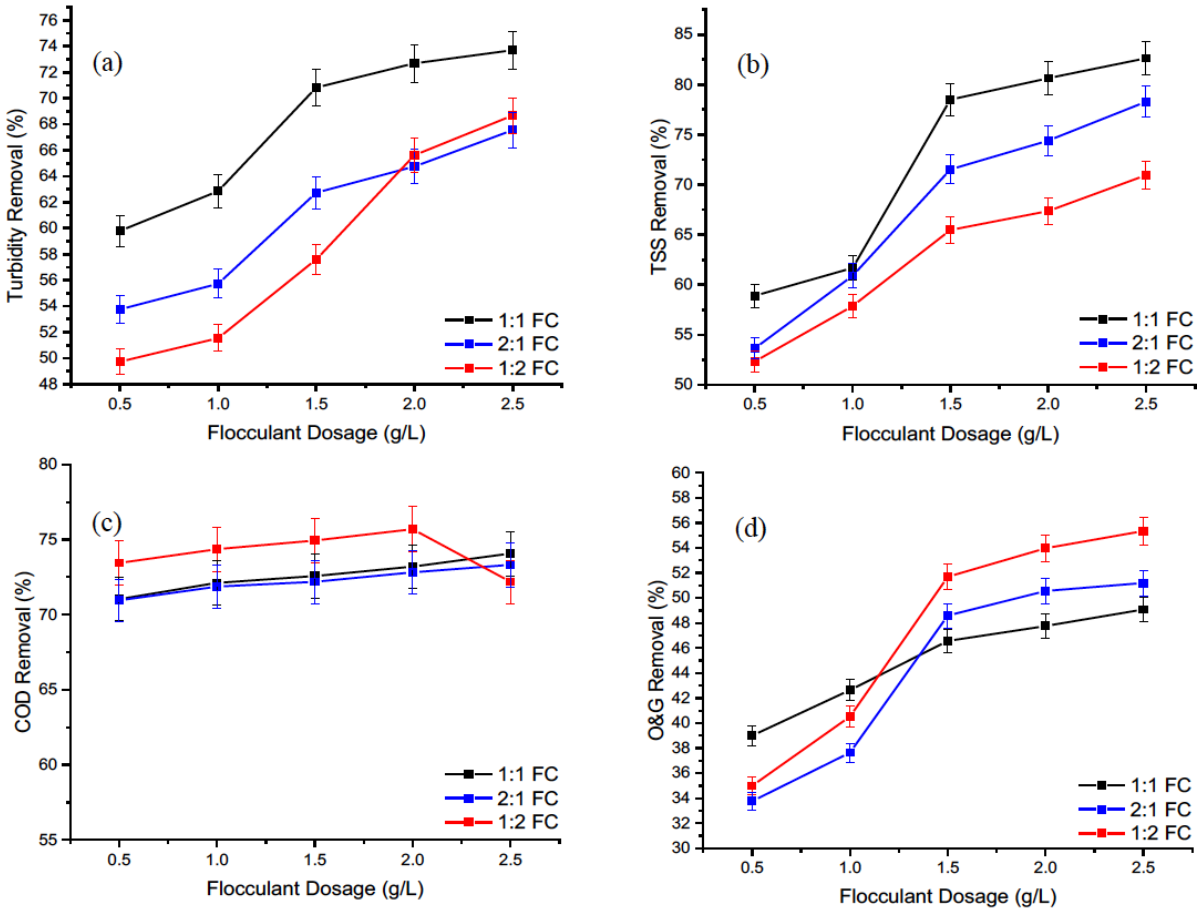

Figure 1: Effect of dosage on percentage removal of (a) turbidity, (b) TSS, (c) COD and (d) O&G (pH = original POME, settling time = 75 min)

The results indicate a proportional increase in the percentage removal of contaminants with the elevation of flocculants dosage until reached a peak value. Beyond this optimum point, there is a slight exacerbation in performance decline with each additional dose of flocculants. This phenomenon is attributed to the gradual weakening of the repulsive forces between particles as the charge neutralisation point is approached, as proposed in the flocculation mechanism based on charge neutralisation by Maćczak et al. [11]. Moreover, the trends observed in turbidity and TSS were found to be similar (Figures 1(a) and 1(b)), albeit with varying percentages of removal for each ratio of derivative iron oxide-chitosan nanocomposites under investigation. Ahmadi and Izanloo [12] suggest that the calibration relationships between turbidity and TSS exhibit excellent linearity, closely passing by the origin. In simpler terms, the turbidity level is shown to increase directly in proportion to the rise in TSS in the sample. This correspondence in trends provides valuable insights into the interplay between flocculants dosage, charge neutralisation and the removal efficiency of contaminants in the flocculation process.

The data presented in Figure 1 reveals a notable increase in the percentage removal of contaminants after the 1.5 g L^{-1} dosage, showing an improvement of approximately 5 % compared to the pre-treatment removal percentage of 14 %. This finding underscores the significance of optimising flocculant dosage to enhance treatment efficiency while avoiding overdosing, which could potentially diminish system efficacy. The observed phenomenon is believed to be associated with the reversal of surface charge and the subsequent destabilisation of flocculant particles. Exceeding the saturation level of polymer bridging due to an overdose of flocculants can lead to the disruption of polymer bridging between particles. This disruption, as explained by Noor et al. [13], has the potential to elevate the concentration of contaminants in the water supply. Adjimani and Asare [14] emphasised that overloading iron oxide-chitosan flocculants may decrease flocculation performance efficacy. This could be attributed to the excess presence of Fe^{2+} and Fe^{3+} in the solution, acting as electron scavengers for the generated hydroxyl radicals. Thus, careful consideration of flocculant dosage is crucial for optimising performance and avoiding potential adverse effects on the flocculation process.

In the current study, the application of the derivative FC nanocomposites revealed distinct performances based on different ratios. Specifically, the 1:1 FC ratio demonstrated the most effective removal, achieving the highest percentage reductions at a settling time of 75 min. This resulted in substantial removal percentages of 74.52 % for turbidity, 81.79 % for TSS, 73.88 % for COD and 47.63 % for O&G, surpassing other ratios. Conversely, the 2:1 FC ratio exhibited the least reduction in turbidity, TSS, COD and O&G at the same settling time, with values of 67.48 %, 78.82 %, 73.52 % and 50.96 %, respectively. The overall flocculation performance, considering the reduction of parameters, followed the order of 1:1 FC > 1:2 FC > 2:1 FC.

3.2 FTIR Analysis

In the previous section, it was established that the 1:1 FC ratio resulted in the highest percentage removal of contaminants in the treated POME. Consequently, the subsequent characterisation studies (FTIR, EDX and OPM) were specifically focused on 1:1 FC nanocomposite to gain more in-depth understanding of its properties and performance.

The chemical bonding nature of ferrihydrite, chitosan and FC nanocomposite is represented by Figure 2. Figure 2(a) revealed three distinct signals in the ferrihydrite spectrum. Firstly, a broad band at 3150 cm^{-1} was observed, corresponding to the OH stretching signal, associated with both structural hydroxide and adsorbed H_2O. Additionally, a deformation water bending vibration near 1650 cm^{-1} was noted, along with the asymmetric and symmetric stretching of C-O from adsorbed carbonate at 1458 and 1336 cm^{-1}. The FTIR spectrum of chitosan (Figure 2(b)) reveals several distinctive absorption bands, each corresponding to specific molecular vibrations and functional groups. The spectrum exhibits a broad and strong band at 3406 cm^{-1}, which can be attributed to the stretching vibration of –OH groups, the extension vibration of N-H, and intermolecular hydrogen bonds of polysaccharides. These signals are considered the main characteristic features identifying chitosan. The absorption bands

at 2890 and 2819 cm^{-1} are assigned to the asymmetric and symmetric $–CH_2$ stretches, respectively. Additionally, typical frequencies for –NH bending vibrations of primary amine groups are observed in the FTIR spectra of chitosan, appearing at 1640 and 1580 cm^{-1}. Each of these peaks and bands contributes to the comprehensive characterisation of chitosan and its molecular structure.

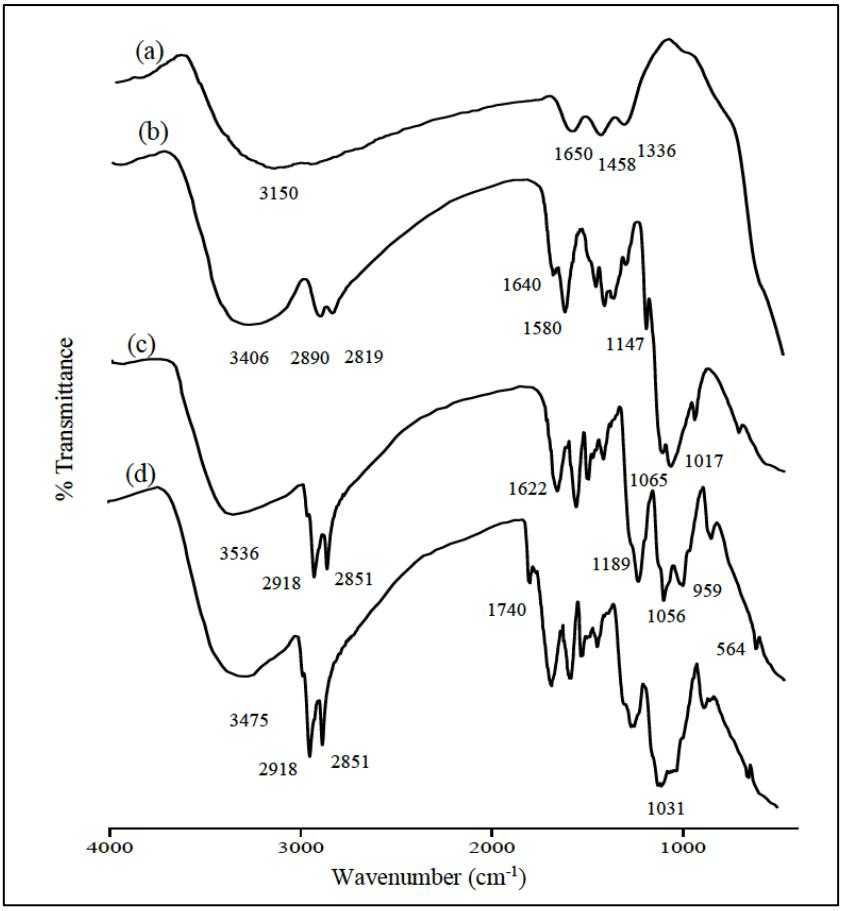

Figure 2: FTIR spectra (a) ferrihydrite, (b) chitosan, (c) 1:1 FC before POME treatment and (d) 1:1 FC after POME treatment

The FTIR spectrum after the synthesis of the FC nanocomposite revealed significant changes when compared to the spectra of the precursor materials. The spectrum exhibited a merging of two precursor materials, indicating a considerable similarity between them. For instance, the two distinct bands at 1640 and 1580 cm^{-1}, corresponding to the –NH bending vibration of the primary amine group in cross-linked chitosan, transformed into a single peak 1622 cm^{-1} after the coupling of chitosan with ferrihydrite nanoparticles (Figure 2(c)). This change is consistent with findings in studies by Li et al. [15], where the disappearance of these peaks was attributed to the chelation of amino groups with the iron oxide nanoparticles in the sample solution. Additionally, the peak related to –NH at 1640 cm^{-1} (Figure 2(b)) shifted towards lower wavenumbers, specifically to 1622 cm^{-1} (Figure 2(c)). This shift indicated potential interactions between the $–NH_2$ group of chitosan and the –O or –OH group of ferrihydrite. Further evidence supporting this interaction was observed in the shifted and changed band associated with the –OH deformation of chitosan at 3406 cm^{-1} (Figure 2(b)). The interaction between ferrihydrite nanoparticles and the hydroxyl and amine groups of the chitosan skeleton was proposed to occur through hydrogen bonding, as suggested by Chandrakumara et al. [16]. Importantly, the introduction of ferrihydrite into the chitosan matrix was substantiated by the appearance of a new absorption peak at 564 cm^{-1} in the FC nanocomposite spectrum (Figure 2(c)). This peak is attributed to the Fe-O stretching of ferrihydrite, providing evidence for the successful composite formation of ferrihydrite within the chitosan matrix.

Following the flocculation treatment process, notable changes were detected in the FTIR spectrum of the FC nanocomposite. First, the absorption intensity peaks at 2918 and 2851 cm^{-1}, attributed to the aliphatic methylene group stretching, were observed to increase after flocculation treatment with POME (Figure 2(c)). This change can be associated with the presence of fatty acids and lipids in POME, as the C-H stretching of aliphatic structures is indicative of these compounds. Fats, oils, and lipids are characterised by a repetition of methylene groups [14]. Additionally, a new absorption band at 1740 cm^{-1} appeared in the FTIR spectra after flocculation (Figure 2(d)), serving as evidence of the interaction between POME and FC nanocomposite. This novel peak, attributed to carbonyl ester groups, is associated with the oil present in POME. Ganapathy et al. [17] highlighted that the carbonyl ester functional group is commonly identified in oil-based media. Furthermore, the intensity of the characteristic peak at 1650 cm^{-1}, related to the stretching of the carbonyl group, increased. This suggests the presence of the carbonyl group in POME. Additionally, the C-O stretching vibration bands at 1056 and 959 cm^{-1}, initially displaying two sharp peaks (Figure 2(c)), changed to a single broad peak. This alteration may be explained by the disappearance of bands due to loosely bound material in the FC nanocomposite after flocculation treatment. Heteroatoms composed of oxygen and nitrogen is believed to remain on the carbon layer [15].

3.3 EDX Analysis

In Figure 3, the EDX spectra of the 1:1 FC nanocomposite before and after POME treatment are presented. The pre-nanocomposite analysis showed the presence of Fe and O compositions, corresponding to ferrihydrite nanoparticles. However, after the composite process, a new C and N peak emerged, indicating the presence of chitosan particles (Figure 3(a)). Carbon, nitrogen, and oxygen are the three primary elements of the chitosan structure, and their binding energy levels in EDX spectra are approximately 0.2, 0.4, and 0.5 keV, respectively (Figure 3(a)).

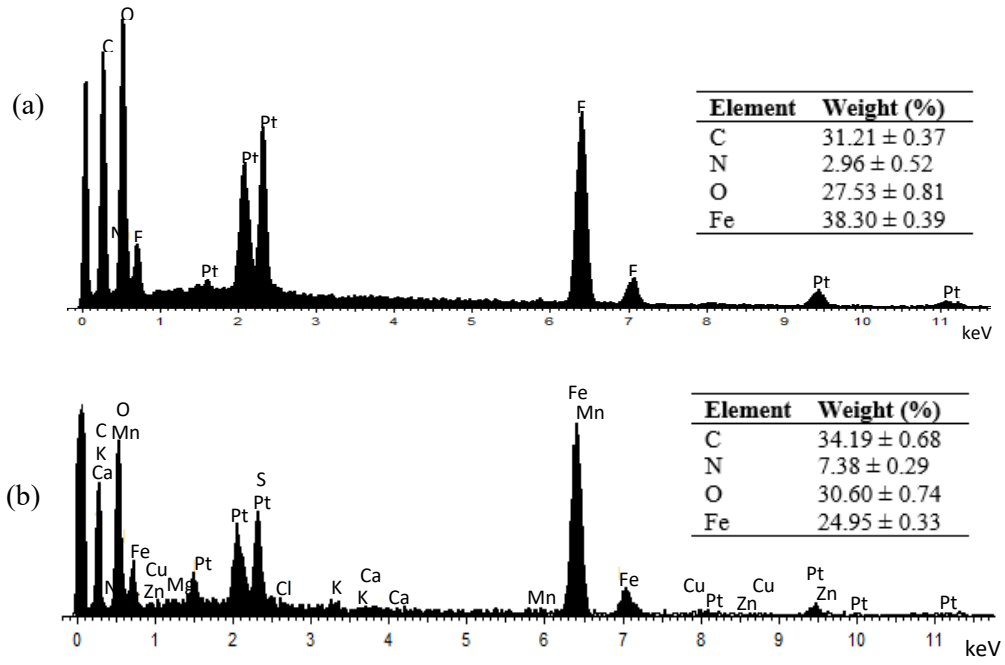

Figure 3: EDX spectra (a) 1:1 FC before POME treatment and (b) 1:1 FC after POME treatment

The appearance of new energy binding features for carbon and nitrogen in the EDX spectra is consistent with the incorporation of chitosan into the iron oxide nanoparticles. This might indicate a successful bonding between iron oxide and chitosan particles. The interaction of these two components has resulted in the emergence of carbon and nitrogen features in all four samples studied. Overall, the

EDX spectra findings support the conclusion that iron oxide and chitosan particles have been successfully bonded together in the formation of the nanocomposite, as discussed previously in FTIR analysis (Section 3.2).

After POME treatment, the EDX spectra exhibit new peaks for Mg, S, K, Ca, Mn, Cu, Zn, and other elements (Figure 3(b)). Additionally, there is an apparent increase in the percentage weights of C, N, and O elements, while the percentage weight of the Fe element appears to decrease after the treatment which mainly due to surface masking by adsorbed contaminants. These changes suggest an interaction between the POME contaminant and the nanocomposite, indicating that the contaminant has been detected on the surfaces of the synthesised nanocomposites. This observation aligns with the expected behaviour, and the results of the EDX investigation suggest that the synthesised nanocomposites have the capability to neutralise the polluting ions in POME waste.

3.4 OPM Analysis

In this study, OPM analysis is employed to identify unknown contaminant particles in effluent. This method enables the identification of particles through the observation of their shape and optical properties, including birefringence and refractive index, using techniques such as dispersion staining [18]. Figure 4 presents OPM images of raw and treated POME using an FC nanocomposite at a 1:1 ratio (w/w). These images are used to analyse the shape and size of the particles after the completion of the flocculation treatment.

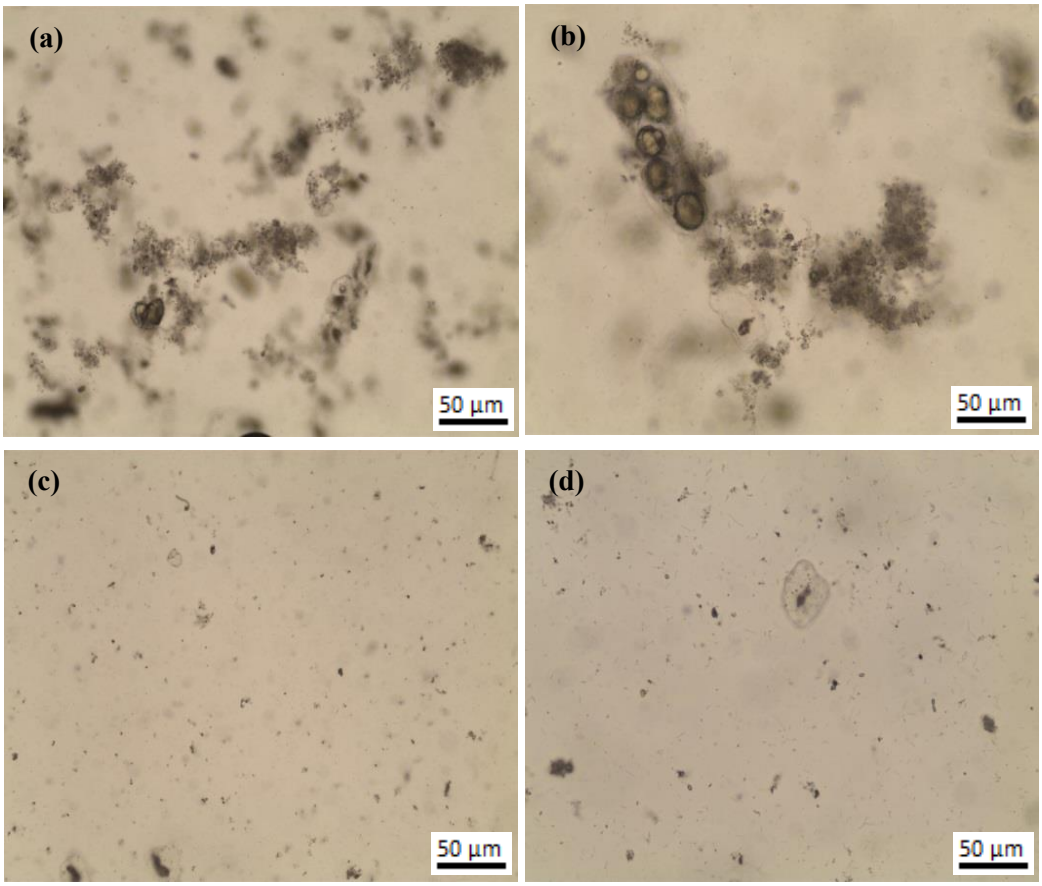

Figure 4: Birefringence of (a-b) raw POME at magnification x10 and x20, and (c-d) treated POME using 1:1 FC at magnification 10x and 20x

The analysis of OPM images revealed distinct differences in the particle size of contaminants in raw POME. At a magnification of 20 times, the raw POME image shows clusters of circles and a dark aggregated particulate matter (Figure 4(b)). According to interpretations, the clusters of circles

represent oil, while the dark clouds symbolise palm fruit residue commonly found in the effluent from the palm oil industry [19,20]. As known from the literature, POME is mainly composed of three major components: water, oil, and suspended solids, with the latter consisting primarily of detritus from the fruit. Interestingly, the OPM analysis after the flocculation treatment revealed a significant decrease in particle size (Figures 4(c) and 4(d)). The image suggests that the nanocomposite has great potential for use in the treatment of industrial wastewater, indicating effective removal or aggregation of contaminants from the effluent.

4. CONCLUSIONS

POME is naturally an acidic and suspended effluent, and the application of FC nanocomposites emerges as a promising method to destabilise the pollutants within POME. The synthesised FC nanocomposites exhibit an additive effect, demonstrating the simultaneous removal of multiple contaminants present in the effluent. The capability of FC nanocomposites is highly attributed to the presence of amine group in chitosan and the positively charged nature of iron oxide. These features facilitate the destabilisation and adsorption of negatively charged contaminants in POME. Overall, results highlight the feasibility of using FC nanocomposites as effective flocculants for POME. Further research could explore scalability and application in real-world industrial settings.

Acknowledgements

The authors express their sincere gratitude to FGV Palm Industries Sdn. Bhd., Sungkai, Perak, Malaysia for providing POME samples and provision of research facilities.

Author Contributions

All authors contributed toward designing research framework, conducting experiments, interpreting data, drafting and critically revising the manuscript, and agree to be accountable for all aspects of the work.

Disclosure of Conflict of Interest

The authors have no disclosures to declare.

Compliance with Ethical Standards

The work is compliant with ethical standards.

References

[1] Raji, Y. O., Othman, M. H. D., Puteh, M. H., Jasman, S. M., Jaafar, J., Rahman, M. A., Ismail, A. F., Salisu, M, Heng, J., Gunawan, T. & Majid, Z. A. (2026). Photocatalytic treatment of final discharge palm oil mill effluent (POME) using dual-layer hollow fiber ceramic membranes with TiO-embedded mullite: Performance evaluation and mechanistic insights. *Materials Science and Engineering:B*., 323(A), 118695.

[2] Jumadi, J., Kamari, A., Rahim, N. A. & Sapie, S. R. (2023). Phytotoxicity effect study on *Vigna radiata* as affected by variation of palm oil mill effluent (POME) concentration. *AIP Conference Proceedings*, *2556*, 040003.

[3] Salehmin, M. N. I., Tiong, S. K., Mohamed, H., Zainal, B. S., Lim, S. S., Yasin, N. H. M. & Zakaria, Z. (2023). Sustainable bioenergy from palm oil mill effluent: advancements in upstream and downstream engineering with techno-economic and environmental assessment. *Journal of Industrial and Engineering Chemistry*, *133*, 122-147.

[4] Yan, S. J., Chan, Y. J., Thangalazhy-Gopakumar, S., Tiong, T. J. & Lim, J. W. (2025). Optimizing anaerobic digestion of palm oil mill effluent (POME) with biochar: Synergistic impact of biochar addition and kinetic analysis. *Journal of Water Process Engineering*, *70*, 106919.

[5] Ahmad, I., Ibrahim, N. N. B., Abdullah, N., Koji, I., Mohamad, S. E., Khoo, K. S., Cheah, W. Y., Ling, T. C. & Show, P. L. (2023). Bioremediation strategies of palm oil mill effluent and landfill leachate using microalgae cultivation: An approach contributing towards environmental sustainability. *Chinese Chemical Letters*, 34(5), 107854.

[6] Zhang, Y., Li, H., Jiang, Q., Jiang, S., Wang, Y. & Wang, L. (2021). One-pot synthesis of a novel P-doped ferrihydrite nanoparticles for efficient removal of Pb(II) from aqueous solutions: Performance and mechanism. *Journal of Environmental Chemical Engineering,* 9(4), 105721.

[7] Zhang, R. & Xu, H. (2023). Environmental properties and applications of cellulose and chitin-based bionanocomposites. In *Biodegradable and Environmental Applications of Bionanocomposites*, Ed. Visakh, P. M. (Springer, Cham), pp. 99-140.

[8] Keshavarz, L., Ghaani, M. R. & English, N. J. (2021). The importance of precursors and modification groups of aerogels in CO_2 capture. *Molecules*, 26(16), 5023.

[9] Jumadi, J., Kamari, A., Rahim, N. A., Yusof, N., Sutapa, I. W. & Sunardi, S. (2024). Ferrihydrite-chitosan nanocomposite as a recyclable flocculant for palm oil mill effluent. *Jurnal Teknologi*, 86(2), 169-182.

[10] Saritha, V., Srinivas, N. & Vuppala, N. V. S. (2017). Analysis and optimization of coagulation and flocculation process. *Applied Water Science*, 7(1), 451-460.

[11] Maćczak, P., Kaczmarek, H. & Ziegler-Borowska, M. (2020). Recent achievements in polymer bio-based flocculants for water treatment. *Materials*, 13(18), 3951.

[12] Ahmadi, S. & Izanloo, C. (2023). Biosynthesis of iron oxide nanoparticles at different temperatures and its application for the removal of Zinc by plant mediated nanoparticle, as an eco-friendly nanoadsorbent. *Results in Chemistry,* 6, 101192.

[13] Noor, M. H. M., Lee, K. J. & Ngadi, N. (2021). Starch engineered with *Moringa oleifera* seeds protein crosslinked Fe_3O_4: A synthesis and flocculation studies. *International Journal of Biological Macromolecules*. 193(B), 2006-2020.

[14] Adjimani, J. P. & Asare, P. (2015). Antioxidant and free radical scavenging activity of iron chelators. *Toxicology Reports. 2*, 721-728.

[15] Li, J., Li, Z., Song, Y., Zhang, X., Xie, H., Sheng, S. & Zou, H. (2024). 3D/1D Fe_3O_4@TiO_2/TC-TiO_2/SiO_2 magnetic inorganic-framework molecularly imprinted fibers for targeted photodegradation. *Inorganic Chemistry*, 63(23), 10568-10584.

[16] Chandrakumara, G. T. D., Dissanayake, D. M. S. N., Mantilaka, M. M. M. G. P. G., De Silva, R. T., Pitawala, H. M. T. G. A. & de Silva, K. M. N. (2019). Eco friendly, green packaging materials from akaganeite and hematite nanoparticle-reinforced chitosan nanocomposite films. *Journal of Nanomaterials*, *2019*, 1-11.

[17] Ganapathy, B., Yahya, A. & Ibrahim, N. (2019). Bioremediation of palm oil mill effluent (POME) using indigenous *Meyerozyma guilliermondii*. *Environmental Science and Pollution Research*, 26(11), 11113-11125.

[18] Wu, H. & Qiao, Y. (2021). Microscopy techniques for protocell characterization. *Polymer Testing*. 93, 106935.

[19] Nursyairah, J., Lau, H. L. N. & Loh, S. K. (2026). Improvement of cold filter plugging point of biodiesel blends with selected additives. *Biofuels*, 17(3), 447-460.

[20] Xuan, T., Hou, C., Chen, X., Zhang, W., Zhang, Y., Dai, T., Liu, R., Zhang, Y. & Zhang, X. (2026). Effects of high-energy fluidic microfluidizer treatment on the physical stability, quality optimization and antioxidant activity of whole jackfruit (*Artocarpus heterophyllus* Lam.) slurry. *LWT – Food Science and Technology*, 242, 119117.